MULTI SENSOR AIRBORNE SYSTEMS: THE POTENTIAL FOR IN SITU SENSOR CALIBRATION

N. Yastikli[a] *, C. Toth[b], D. Brzezinska[c]

[a] YTU, Department of Geodetic and Photogrammetric Engineering, 34349, Istanbul, Turkey - ynaci@yildiz.edu.tr
[b] Center for Mapping , Ohio State University, Columbus Ohio, 43212 USA - toth@cfm.ohio-state.edu
[c] Department of Civil and Environmental Engineering and Geodetic Science, Ohio State University, Columbus Ohio, 43210, USA - grejner-brzezinska.1@osu.edu

KEY WORDS: LiDAR, Digital Camera, GPS, IMU, Sensor, Orientation, Calibration.

ABSTRACT:

Airborne LiDAR systems are integrated with a positioning and orientation system including GPS (Global Positioning System) and INS (Inertial Navigation System) to measure the exterior orientation of the sensors. LiDAR systems are frequently integrated with digital cameras in recent years. The digital camera imagery is directly oriented by using the platform navigation solution of the integrated GPS and IMU system. The direct sensor orientation approach, used for georeferencing of imaging sensors, is more sensitive to calibration errors, and therefore, the calibration of individual sensors and the relation between sensors (system calibration) is critical for accurate georeferencing. In addition, the physical parameters during the flight mission may differ from assumed calibration parameters, causing errors in object space for any products derived from the imagery; the calibration of digital cameras as well as laser sensor is usually performed in laboratory conditions. The displacement vectors between GPS, INS and imaging sensors, such as digital camera and LiDAR should be determined as well as their attitude relationship. The boresight misalignment, the determination of the displacement vector and attitude relationship between sensors is critical and requires a test field with distributed control points of high accuracy where adequate data can be collected for the parameter determination. Finding such a test field nearby or within project area, however, is not always possible. On the other hand, the multi sensor environment could provide redundant object space information that potentially could be exploited for certain calibration and QA/QC processes. This paper aims to share our experiences obtained by in situ calibrating a digital camera using LiDAR data. The multi sensor system included the small format Redlake MS 4100 RGB/CIR digital camera and the Obtech 3100 ALSM, supported by the Applanix georeferencing system (Novatel GPS and LN200 IMU). The investigation focused on determination of in-situ determined camera and boresight calibration parameters based on using only the LiDAR data acquired in the project. The performance of the determined in-situ camera calibration parameters and boresight misalignment were analyzed by comparing the results of measuring points in stereo models formed using bundle block adjustment and direct sensor orientation, respectively for multi sensor system. The performance of multi sensor orientation was also tested using independent LiDAR-specific target points which were originally used for testing of the LiDAR data accuracy. In addition, the effect of orientation discrepancies as a model deformation was also checked by computing y-parallaxes and generated orthoimage.

1. INTRODUCTION

The laser scanning is a mature technology, with the integration of the fields in optics, opto-mechanics and electronics. Airborne LiDAR systems are fully accepted in surveying and mapping community since mid-1990's, which supply us the X,Y,Z coordinates of the locations of a footprint of a laser beam in 3D space with high accuracy as well as intensity data . The positioning and orientation system including GPS (Global Positioning System) and INS (Inertial Navigation System) is integrated with the Airborne LiDAR systems. The accuracy of the X, Y, Z coordinates of the laser footprints on the target surface depend on the sensor orientation parameters from GPS and IMU and range measurements from airborne LiDAR.

In recent years, digital cameras are frequently integrated with Airborne LiDAR system to allow for visual coverage and to improve the mapping performance of the multi sensor system. The orientation of images acquired by digital camera in integrated system is performed by the platform navigation solution from GPS and IMU system.

In photogrammetry, the determination of image orientation, solved indirectly by block adjustment. In multi sensor airborne system, such as LiDAR, digital camera, GPS and IMU, the direct determination of the exterior orientation parameters of imaging sensors is performed by the combined use of IMU and GPS. For accurate determination of object points based on GPS/IMU oriented imagery, the system calibration is of vital importance, and includes the determination of the boresight misalignment, the interior camera orientation, and the GPS antenna offset. The system calibration procedure includes the calibration of individual sensors and the calibration between sensors. The calibration between sensors is comprised of the GPS antenna offset (lever arm), and the determination of an offset vector and attitude difference between the IMU body frame and the imaging sensor. The accurate calibration of multi-sensor airborne systems, including digital camera, LiDAR,

---

* Corresponding author

GPS, IMU, etc, is of high importance, since sensor orientation is very sensitive to changes in sensor geometry because of the extrapolation from the camera projection center to the ground. The camera calibration process involves the geometric calibration, resolution determination and radiometric calibration of camera. The laboratory calibration is a standard method for analog airborne frame cameras and the interior camera geometry, i.e. focal length, principle point location and lens distortion parameters are estimated. In-situ calibration, also called self-calibration originates from close range applications and requires a large number of signalized control points in 3D terrestrial calibration fields. The airborne in-situ calibration also requires a calibration field with signalized control points of high accuracy. The focal length, principle point location and lens distortion parameters are estimated during the calibration process from the measurements reflecting actual conditions.

The ASPRS and the EUROSDR continue their research on digital camera calibration and validation (Stensaas, 2005, Cramer, 2005). The lab calibration method is still used for geometric calibration of large format digital cameras such as ZI Imaging DMC and Leica ADS40 together with in-situ calibration (Dörstel et al., 2003, Tempelmann, et al., 2003). For medium format digital cameras such as the Applanix/Emerge DSS geometric calibration is done by terrestrial and airborne calibration (Mostafa, 2004). The terrestrial in-situ calibration method is used for geometric calibration of the Vexcel Ultracam$_D$ large format digital camera (Kröpfl, et al, 2004). The U.S. Geological Survey (USGS) began its certification efforts with digital aerial cameras in January 2006 (Stensaas, 2006). Current investigations at USGS focus on geometric and spatial characterization and calibration, although research on radiometric characterization and calibration of airborne sensors also continues with the recently established digital camera calibration lab at the USGS Center for Earth Resources Observation and Science (EROS). To perform in-situ camera calibration, a calibration range was established also at USGS EROS with 150 surveyed panels and one CORS station (http://calval.cr.usgs.gov).

The offset between the GPS antenna and the IMU or imaging sensor can be precisely measured by conventional survey methods. The boresight misalignment is determined by a comparison of the GPS/IMU derived image orientation with the results of a bundle block adjustment over a calibration field containing control points. Finding such a calibration field nearby or within project area, however, is not always possible.

This research was motivated by the circumstances of a LiDAR mapping project, where a small format digital camera was installed next to the LiDAR system in the last minute before the airborne surveys started. There were no measurements and no dedicated data acquisition performed to support boresight calibration of the camera except for an earlier lab camera calibration. Furthermore, there was no target range or any area with signalized controls in the project area. Therefore, this investigation aimed to determine the system calibration parameters for that multi sensor airborne system using only the LiDAR data acquired in the project. The multi sensor airborne system included the small format Redlake MS 4100 RGB/CIR digital camera and the Obtech 3100 ALSM, supported by the Applanix georeferencing system (Novatel GPS and LN200 IMU). Experiments with the data set and the results obtained are analyzed and discussed to assess the performance of system calibration for the Redlake MS 4100 camera.

2. PROJECT AREA AND DATA ACQISITION

The data set from the project B4 Airborne Laser Swath Mapping (ALSM) survey of the San Andreas Fault (SAF) System of Central and Southern California, including the Banning Segment of the SAF and the San Jacinto Fault system was used (Toth et al., 2007). The project B4, codenamed to reference to the "before" status of a widely anticipated major earthquake, the Big One, is a National Science Foundation (NSF) sponsored project, led by scientists from The Ohio State University (OSU) and the U.S. Geological Surveys (USGS), to create an accurate surface model (DEM) along the San Andreas and San Jacinto Faults in southern California. Besides the USGS, the OSU-led team included NCALM (National Center for Airborne Laser Mapping) from the University of Florida, UNAVCO (a non-profit, membership-governed consortium, supporting Earth science) and Optech International.

The airborne surveys took place May 15-25, 2005 with a Cessna 310 aircraft which was hired and Optech International provided the ALTM 3100 system. The state-of-the-art Optech 3100 system was configured for 70 kHz, resulting in an about 2 pts/m^2 LiDAR data. An experimental Redlake MS 4100 digital camera was installed next to the Optech 3100 system, providing imagery of 1K by 2K resolution in four bands. The images were captured at 1 Hz, synchronized to the 1PPS GPS signal. The project area, encompassing about 1,000 km of fault line, was segmented into smaller sections during flight planning, including the San Andreas and San Jacinto Fault lines.

3. GEOMETRIC CALIBRATION

An experimental digital camera used in this project was the Redlake MS 4100 RGB/CIR digital camera, which has four CCD sensors each with 1920 x 1075 pixels and pixel size of 7.4 μm x 7.4 μm. The laboratory camera calibration was performed in RGB mode and a focal length was estimated for 25.966 mm in the calibration report. The calibration values were used as initial calibration parameters for the in situ calibration of the Redlake MS 4100 camera. The camera was configured for CIR image capture for the airborne surveys. The CIR imagery has 1892 x 1060 pixels, different from the RGB images. The approximate image size is 8 mm in the flight direction and 14.2 mm across the flight direction.

A reference block was selected from a typical flight on May 25, 2005 with 21 images, where several man-made structures were available (Figure 1). 25 control points were used to perform an airborne in-situ calibration of the Redlake MS 4100 digital camera which were extracted from the LiDAR point cloud and intensity data (Figure 2).
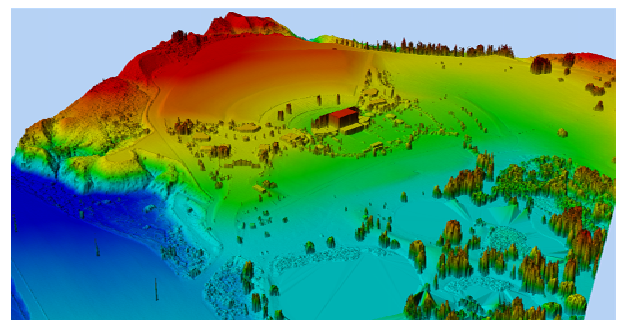

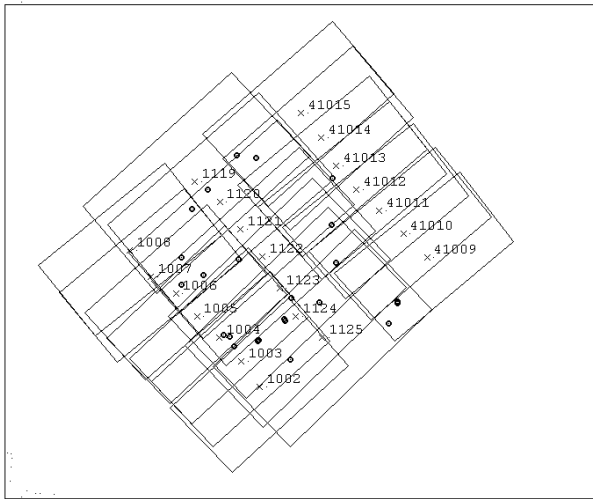**Figure 1**. The 3D view of geo-registered LiDAR point clouds

Figure 2. The reference block and control points distribution

The availability of good control points is a crucial requirement for in-situ calibration. The control points were derived from the LiDAR point cloud using LiDAR intensity as a tool for point identification, since no conventional control points were available in this project. An example for derived control point in the CIR image and in LiDAR intensity image can be seen in Figure 3. The expected root means square error of LiDAR points is about $\pm$ 10 cm all component (Csanyi and Toth, 2007).
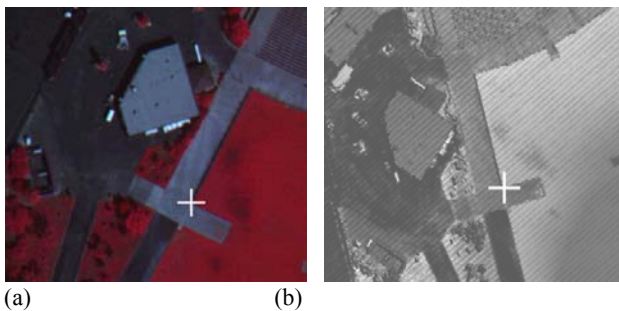

(a)   (b)

Figure 3. The derived control points from the LiDAR point cloud in CIR image (a) and intensity image (b)

The block was flown in approximately 650 m above ground, corresponding to an image scale 25300 and the height to base relation is about 10 for an average endlap of 68%. In other words, the 17.5^o view angle in the flight direction with is very small comparing to the normal analog camera, which is 73.9^o at the 153 mm focal length. The small view angle in the flight direction requires more images in the flight lines, but more importantly, it significantly reduces the Z accuracy of the determined object points.

The different sets of the system calibration parameters were computed to analyze the estimated system calibration parameters using the BLUH bundle block adjustment software from the University of Hannover. The various combinations of the adjustment runs with different parameters and results are given in Table 1. The focal length f = 25.966 from the USGS/EROS calibration report was used as initial value in Table 1 for first two approaches. The twelve additional parameters were introduced to block adjustment in the second

approach (Jacobsen, 2006). The radial symmetric lens distortions and systematic image errors are determined with additional parameters introduced into the block adjustment. The radial systematic lens distortions from both the USGS/EROS calibration report and the bundle block adjustment are shown in Figure 4 and Figure 5. The systematic image errors of the Redlake MS 4100 digital camera were also determined with introduced additional parameters as shown in Figure 6.

	Approach	σ_0 [μm]	RMS at Control Points [m]		
			X	Y	Z
1	Bundle block adjustment	5.5	0.33	0.33	1.28
2	Bundle block adjustment with 12 add parameters	4.3	0.31	0.23	0.25
3	GPS supported bundle block adjustment with 13 additional parameters	5.2	0.33	0.23	0.51
4	Bundle block adjustment with improved image coordinate and focal length	4.3	0.31	0.23	0.24
5	GPS supported bundle block adjustment with improved image coordinate and focal length	5.4	0.34	0.23	0.55

Table 1. Reference bundle block adjustment results in UTM

The correction for the focal length was 123 μm with introduced additional parameter to the bundle block adjustment in third approach. The affine model deformation of UTM system in this test area was causing a 10 μm correction for the focal length (Yastikli et al., 2005). The remaining part of the correction for the focal length could be explained by the effect of actual flight condition such as air pressure and temperature. The additional parameters for the location of principle point were not introduced to the adjustment because the strips, which were flown in twice in opposite directions, were not available in the reference block. The corrected focal length, however, resulted in improved image coordinates, including new radial symmetric lens distortions and symmetric image errors. The traditional bundle block adjustment and GPS supported bundle block adjustments were repeated with the improved image coordinates and corrected focal length in approaches 4 and 5.
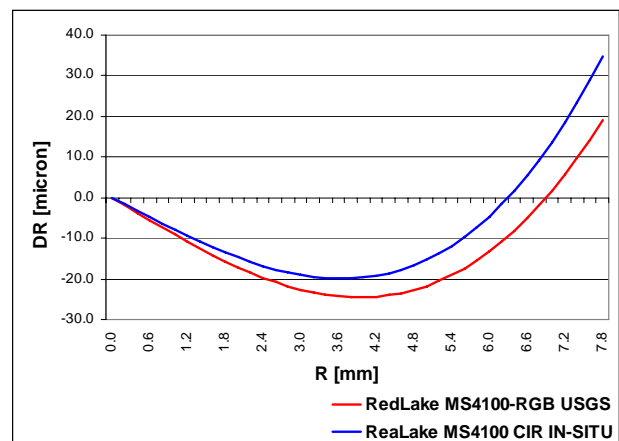

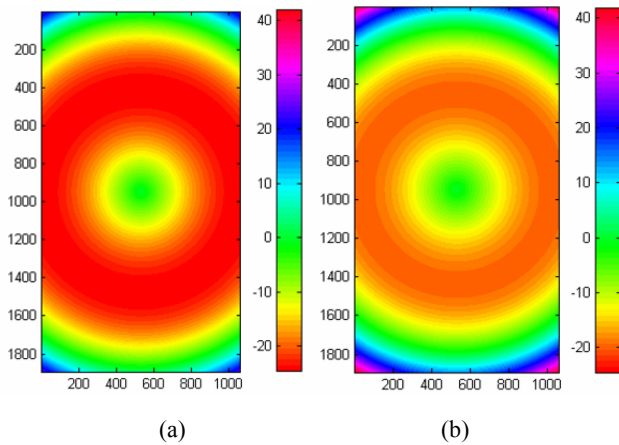**Figure 4.** The radial systematic lens distortion from calibration report and reference block adjustment

Figure 5. The radial systematic lens distortion in the image from calibration report (a) and in-situ calibration (b) (μm)
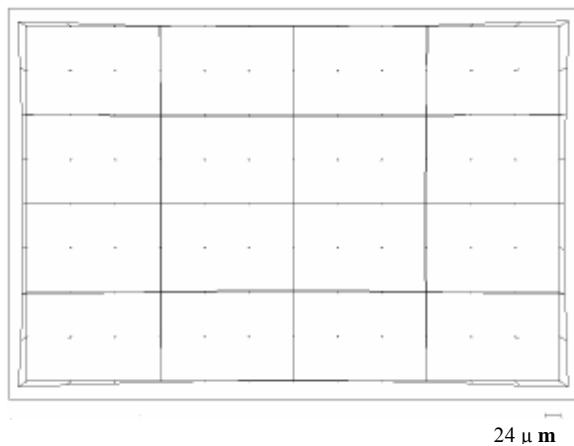

Figure 6. Systematic image errors determined by introduced additional parameters to the reference adjustment

4. BORESIGHT MISALIGNMENT

The image orientation determined by GPS-supported bundle block adjustment, with improved image coordinate and focal length in approach 5 was used for the determination of the boresight misalignment. The orientations from the GPS-supported bundle block adjustment were compared to the orientations obtained from GPS/IMU processing. The shift parameters were determined by comparing the projection centers from the reference adjustment to the GPS/IMU-derived projection centers as well as to lever arm measurements.

In general, the IMU is fixed to the camera body as close as possible and is aligned parallel to the camera. In our installation, the camera was installed perpendicular to the flight direction, resulting in a 90° rotation between the x axis of camera and that of the IMU. The orientations from the reference bundle block adjustment were transferred into roll, pitch and yaw and the boresight angles were determined as 0.18476^{o} for roll, 1.29884^{o} for pitch and 0.34447^{o} for yaw. The determined shift values were -0.384 m for X, 0.076 m for Y and 0.050 m for Z.

The boresight angles were also estimated using the POSCal utility of the Applanix POSEO software version 4.1. The

POSCal computation is based on least squares adjustment and the required inputs are the image coordinates, control points and GPS/IMU-derived projection centers and orientations. The 90° rotation between the x axes of the camera and IMU had to be also defined for the computation. The determined boresight angles were 0.16867^{o} for roll, 1.27303^{o} for pitch and 0.40910^{o} for yaw.

The GPS/IMU-derived attitudes and positions were improved by the BLUH and Applanix POSCal boresight misalignment. Based on the improved GPS/IMU derived attitudes and positions, the object coordinates of measured tie points and check points were computed by combined intersection (direct sensor orientation). The 25 control points derived from the LiDAR point cloud were used as check points. The σ_0 of the direct georeferencing and root means square errors at check points can be seen in Table 2.

	Approach	σ_0 [μm]	RMS at Control Points [m]		
			X	Y	Z
1	Direct georeferencing using BLUH boresight misalignment	52.2	1.14	0.79	5.35
2	Direct georeferencing using Applanix boresight misalignment	46.0	1.18	0.70	5.57

Table 2. Direct georeferencing results in UTM

The effect of the orientation discrepancies can be seen as y parallaxes. The y parallax in the model is important for stereo model setup. The comparison of the model y parallaxes from direct sensor orientation based on BLUH and Applanix boresight angles, and GPS supported bundle block adjustment can be seen in Figure 7. The similar results obtained for both direct sensor orientations clearly indicate an unacceptable quality for stereo models.
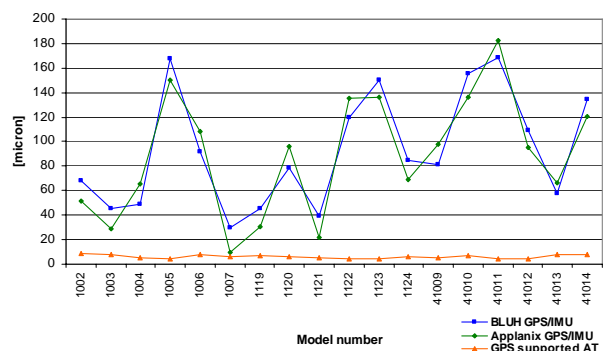

Figure 7. Comparison of the y parallaxes

To further check the quality of the sensor calibration and boresight misalignment, orthoimages were generated using GPS supported bundle block adjustment results and GPS/IMU derived attitudes and positions improved by BLUH boresight misalignment. The effect of orientation discrepancies to the orthoimages can be seen comparing the LiDAR intensity images and the generated orthoimages in Figure 8. The in-situ camera and boresight calibration were determined based on the data collected on May 25, 2005. The performance of the in-situ

Target Number	Day	Model Number	MSE of Intersection [μm]	RMS at Target Points [m]		
				X	Y	Z
43142	May 23	501	59.8	-1.20	-0.09	0.80
43143	May 23	506	30.8	0.39	0.68	2.0
43144	May 23	505	29.6	0.85	1.257	-2.5
47803	May 24	457	48.4	2.44	2.89	4.89
47804	May 24	457	48.4	2.13	2.59	4.28
46465	May 26	199	30.9	0.24	1.54	0.71
46466	May 26	324	53.8	0.56	-0.59	5.82

Table 3. The results of performance check in-situ and camera calibration with LiDAR specific target points

calibration process was tested by using a limited number of target points which were originally used for the validation of the LiDAR accuracy. Figure 9 shows the LiDAR-specific targets, made of trampolines with 2m diameter, and GPS-positioned at cm-level accuracy.
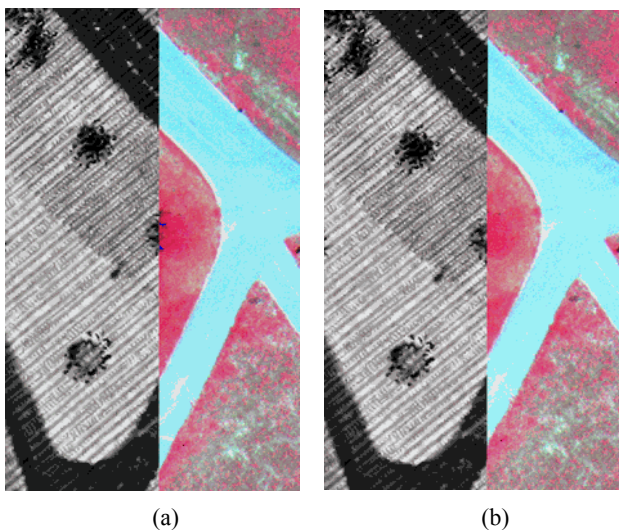

(a)   (b)

Figure 8. The geo-registered LiDAR intensity image and orthoimages based on reference adjustment (a) and direct georeferencing (b).
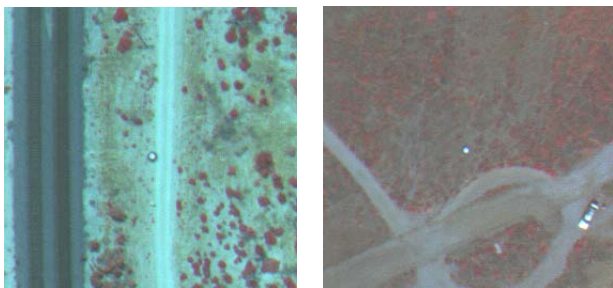

Figure 9. Target points 43142 (a) and 46466 (b)

The image coordinates of check points were measured and the object coordinates were computed by combined intersection (direct sensor orientation). The overall results of the in-situ camera and boresight calibration performance check as a root means square errors at target points are shown in Table 3. The obtained root mean square errors at target points and mean square error of intersection confirmed that the determined in-situ camera and boresight calibration is optimal and stable, as there is not change day to day and from one location to another.

5. CONCLUSIONS

The system calibration of multi sensor airborne systems, including the boresight misalignment and geometric calibration of the imaging sensor has vital importance for achieving accurate geospatial data extraction performance. Any discrepancies between the assumed mathematical model and physical condition during the data acquisition can cause an error in object space. Because of this, the determination of the displacement vector and attitude difference between the camera and IMU body frame (boresight misalignment) and geometric calibration of camera are a critical issue for direct georeferencing.

In this paper, in-situ sensor calibration was performed to integrate a small format camera into a high-performance LiDAR system. The investigation clearly showed that the Redlake MS 4100 digital camera could be successfully calibrated and boresighted to the LiDAR system, using only control information derived from the LiDAR data. Using a block of 21 images and 25 LiDAR-derived control points, bundle block adjustments with various parameters were used to perform an in-situ camera calibration. The focal length, the radial symmetric lens distortions and systematic image errors were accurately estimated (with respect to the camera quality). In addition, the boresight misalignment was simultaneously estimated using the BLUH and Applanix software products. The effect of orientation discrepancies were checked by computing y-parallaxes for each model at the reference block. In addition, an independent performance check was performed using LiDAR-specific ground targets. The combined results clearly proved that the determined in-situ calibration parameters were optimal and stable; in fact, the achieved accuracy appears to be quite good compared to the camera quality.

REFERENCES

Cramer M., 2005. EuroSDR: Digital Camera Calibration and Validation, GeoInformatic 2(8), March 2005, pp. 16-19 .

Csanyi, N. and Toth, C. (2007): Improvement of LiDAR Data Accuracy Using LiDAR-Specific Ground Targets, Photogrammetric Engineering &Remote Sensing, Vol. 73, No. 4, April 2007 pp 385-396.

Dörstel C., Jacobsen K., Stallmann D., 2003. DMC – Photogrammetric Accuracy – Calibration Aspects and Generation of Synthetic DMC Images, in: Grün A., Kahmen H. (Eds.), Optical 3-D Measurement Techniques VI, Vol. I, Institute for Geodesy and Photogrammetry, ETH Zürich, 74-82.

Jacobsen K., 2006. Blim (Program System BLUH) User Manual, Institute of Photogrammetry and GeoInformation, University of Hannover. April 2006.

Kröpfl M., Kruck E. B., M. Gruber A., 2004. Geometric Calibration Of The Digital Large Format Aerial Camera Ultracam$_D$ Proceedings of ISPRS Congress 2004, Istanbul, July 2004, digitally available on CD, 3 pages.

Mostafa, M. 2004. Camera/IMU boresight calibration – new advances and performance analysis
http://www.applanix.com/media/downloads/products/articles_papers/DSS_2004_07_TestResults.pdf (accessed August 28, 2006)

Stensaas G., 2005. Mapping Path to Digital Sensor Calibration, ASPRS Photogrammetry- Part2: Digital Sensor Calibration: Research, Policies and Standards, ASPRS Spring Meeting, March9, 2005, Baltimore, USA.

Stensaas G., 2006. The USGS Plan for Quality Assurance of Digital Aerial Imagery.
http://calval.cr.usgs.gov/documents/The_USGS_and_IADIWG_Plan8.doc (accessed March 28, 2007)

Tempelmann U., Hinsken L., Recke U., 2003. ADS40 calibration and verification process. in: Grün A., Kahmen H. (Eds.), Optical 3-D Measurement Techniques VI, pp. 48-54

Yastikli N., Jacobsen K., 2005 Influence of System Calibration on Direct Sensor Orientation. Photogrammetric Engineering and Remote Sensing, Vol. 71 No 5. May 2005 pp. 629-633.

Toth C., Grejner-Brzezinska, D.A., Csanyi N., Paska E., and Yastikli N., 2007. Lidar Mapping Supporting Earthquake Research Of The San Andreas Fault. *ASPRS Annual Conference – Identifying Geospatial Solutions,* Tampa FL, May 7-11, 2007. CD-ROM.